

[Home](#) [Search](#) [Collections](#) [Journals](#) [About](#) [Contact us](#) [My IOPscience](#)

Direct radiative feedback due to biogenic secondary organic aerosol estimated from boreal forest site observations

This content has been downloaded from IOPscience. Please scroll down to see the full text.

2015 Environ. Res. Lett. 10 104005

(<http://iopscience.iop.org/1748-9326/10/10/104005>)

View [the table of contents for this issue](#), or go to the [journal homepage](#) for more

Download details:

IP Address: 128.214.163.21

This content was downloaded on 13/05/2016 at 08:45

Please note that [terms and conditions apply](#).

Environmental Research Letters



LETTER

Direct radiative feedback due to biogenic secondary organic aerosol estimated from boreal forest site observations

OPEN ACCESS

RECEIVED

28 July 2015

REVISED

5 September 2015

ACCEPTED FOR PUBLICATION

16 September 2015

PUBLISHED

8 October 2015

Heikki Lihavainen¹, Eija Asmi¹, Veijo Aaltonen¹, Ulla Makkonen¹ and Veli-Matti Kerminen^{1,2}¹ Finnish Meteorological Institute, Helsinki, Finland² Department of Physics, University of Helsinki, FinlandE-mail: heikki.lihavainen@fmi.fi

Keywords: aerosol, feedback, biogenic

Content from this work may be used under the terms of the [Creative Commons Attribution 3.0 licence](https://creativecommons.org/licenses/by/4.0/).

Any further distribution of this work must maintain attribution to the author(s) and the title of the work, journal citation and DOI.



Abstract

We used more than five years of continuous aerosol measurements to estimate the direct radiative feedback parameter associated with the formation of biogenic secondary organic aerosol (BSOA) at a remote continental site at the edge of the boreal forest zone in Northern Finland. Our upper-limit estimate for this feedback parameter during the summer period (ambient temperatures above 10 °C) was $-97 \pm 66 \text{ mW m}^{-2} \text{ K}^{-1}$ (mean \pm STD) when using measurements of the aerosol optical depth (f_{AOD}) and $-63 \pm 40 \text{ mW m}^{-2} \text{ K}^{-1}$ when using measurements of the ‘dry’ aerosol scattering coefficient at the ground level (f_{σ}). Here STD represents the variability in f caused by the observed variability in the quantities used to derive the value of f . Compared with our measurement site, the magnitude of the direct radiative feedback associated with BSOA is expected to be larger in warmer continental regions with more abundant biogenic emissions, and even larger in regions where biogenic emissions are mixed with anthropogenic pollution.

1. Introduction

Biogenic secondary organic aerosol (BSOA) originating from the emissions of volatile organic compounds from terrestrial vegetation constitutes an important part of the natural aerosol system. According to large-scale model simulations, the direct and indirect radiative effects of the BSOA are potentially large, yet poorly quantified (Goto *et al* 2008, Spracklen *et al* 2008, O’Donnell *et al* 2011, Rap *et al* 2013, Scott *et al* 2014). This, along with uncertainties in other natural aerosol emissions, seriously hampers our capability to constrain the present-day indirect radiative forcing by anthropogenic aerosols, since this forcing is sensitive to the amount of natural aerosol particles (Carslaw *et al* 2013). Since BSOA precursor emissions are sensitive to temperature and several other environmental variables (e.g. Guenther *et al* 2012), the radiative effects of BSOA are expected to change as a result of future climate change (Kulmala *et al* 2004, Tunved *et al* 2008, Carslaw *et al* 2010). The climate feedbacks resulting from these changes have been investigated to very limited extent so far (e.g. Boucher *et al* 2013).

Complimentary to model simulations, the radiative effects of BSOA can also be estimated by using long-term observations. With help of several years of data on aerosol optical properties measured in Pallas, a site at the northern edge of the boreal forest zone in Finland, Lihavainen *et al* (2009) estimated the radiative effects attributable to BSOA in the regional atmosphere during the summer part of the year. The resulting direct and indirect radiative effects were in the range $-(0.37\text{--}0.74) \text{ W m}^{-2}$ and $-(3.2\text{--}6.4) \text{ W m}^{-2}$, respectively, the latter value range being comparable to the model-simulated estimate obtained by Spracklen *et al* (2008) over the whole boreal forest area. These values can be compared with model-based estimates of the global BSOA radiative effect which span a wide range of values from close to zero up to about -0.8 W m^{-2} for the direct radiative effect and a similar value range for the first indirect radiative effect (Goto *et al* 2008, Rap *et al* 2013, Scott *et al* 2014).

While estimating full feedback loops from observational data is extremely challenging (e.g. Kulmala *et al* 2014), such data can be used to estimate the sensitivity of various radiative forcing components to changes in the ambient temperature. When the ambient

temperature change is driven by climate change, this temperature sensitivity can be interpreted as a climate feedback parameter with the unit $\text{W m}^{-2} \text{K}^{-1}$. Paasonen *et al* (2013) used data from particle number size distribution measurements at 11 terrestrial sites ranging from clean boreal forest environments to polluted background sites, and calculated the temperature-driven feedback parameter by biogenic emissions. The resulting feedback parameter for the indirect radiative effect varied from values close to zero at the polluted sites to values more negative than $-0.1 \text{ W m}^{-2} \text{K}^{-1}$ at the remote sites, with a globally-average estimate equal to $-0.01 \text{ W m}^{-2} \text{K}^{-1}$. The corresponding feedback parameter associated with the direct radiative effect showed mixed results between the different sites, possibly due to uncertainties related to deriving aerosol optical properties based solely on particle number size distribution measurements.

In this manuscript, we will estimate the direct radiative feedback parameter, f , associated with the temperature-dependent BSOA formation at Pallas during the summer period. We base our analysis on long-term observations, more specifically on two independent measurement data sets of aerosol optical properties. The scientific questions we aim to address include: (i) what is the overall magnitude of f in the regional atmosphere and what are the main uncertainties associated with our estimate?, (ii) how does the value of f compare with the corresponding feedback caused by the first aerosol indirect radiative effect?, and (iii) how would we expect f to behave at lower latitudes and in more polluted environments? Besides searching for answers to these questions, we will also discuss briefly what implications our results might have on future studies on this subject.

2. Materials and methods

2.1. Site description

A detailed site description can be found from Hatakka *et al* (2003), so only a short overview is given here. The analysed data have been measured at Pallas-Sodankylä Global Atmosphere Watch (GAW) Station Sammaltunturi measurement site located in Northern Finland ($67^{\circ}58'N$, $24^{\circ}07'E$; 565 m a.s.l.) in subarctic region. The station is hosted by Finnish Meteorological Institute. The station of Sammaltunturi lies on a top of a field, round topped treeless hill, about 300 m above the surrounding area. The timberline lies about 100 m below the station. The region is hilly (250–400 m a.s.l.), forested and partly swampy with some rather large lakes (about 250 m a.s.l.). The station is located inside the Pallas-Yllästunturi National Park (total area 1020 km^2).

Aerosol optical depth (AOD) measurements were made at the Sodankylä observatory in northern Finland ($67.37^{\circ}N$, $26.63^{\circ}E$, 179 m a.s.l.). The observatory is a part of the Pallas-Sodankylä GAW station. The site

is located about 100 km north of the Arctic Circle, ca 125 km SE from Pallas. The station is surrounded by a pine forest. The observatory is emphasized by upper-air weather and ozone soundings, measurements of spectral radiation of UV and total ozone, climatological and other meteorological measurements.

2.2. Measurements

The scattering and backscattering coefficients were measured with an integrating nephelometer (model 3563, TSI, St. Paul, Minnesota). More detailed discussion on scattering coefficient measurements can be found elsewhere (Aaltonen *et al* 2006, Lihavainen *et al* 2009, 2015) and only short description is given here. The instrument measures scattering by aerosols in three wavelengths: 450, 550 and 700 nm. The inlet of the main sampling line is about 3 m above the roof of the station building and about 7 m above the ground. Non idealities due to non lambertian and truncation errors in nephelometer were corrected using the method described by Anderson and Ogren (1998). The nephelometer was calibrated with CO_2 and zero air approximately every other month and the light source was changed every half a year. The zero air calibration was automatically made ones per hour. The measurements were made according to the guidelines of GAW recommendation.

The absorption coefficient was measured with Aethalometer (Magee Scientific, model AE31). The Aethalometer absorption measurement is known to suffer from a filter loading artifact. These artifacts can be corrected using different methods. Here, the approach presented by Weingartner *et al* (2003) was chosen. The particle number size distribution in the range 7–500 nm was measured with a differential mobility particle sizer (DMPS). The instrument and measuring arrangements have been described by Komppula *et al* (2003). The aerosol mass concentration was calculated from the integrated aerosol volume concentrate obtained from the DMPS data multiplied by a density of 1.5 g cm^{-3} . The same methodology was used in earlier studies for our site by Tunved *et al* (2006) and Lihavainen *et al* (2009). Sulfate and other inorganic ions in particles were measured from daily filter samples according to the EMEP-protocol (EMEP, 2007) in Matorova station, 6 km east from Sammaltunturi station.

AOD measurements were made with Precision Filter Radiometer (PMOD, Switzerland), which measures spectral irradiance at 4 separate channels (368, 412, 500 and 862 nm) to obtain AOD. The cloud filter was based on the triplet technique (Smirnov *et al* 2000). The calibration of the instrument was carried out once per year by the manufacturer. The seasonal variability of the AOD in Sodankylä has been discussed by Aaltonen *et al* (2012).

Weather variables were measured with an automatic weather station. The measured variables were

temperature, pressure, relative humidity, and wind speed and direction. At the Sammaltunturi station, there were also sensors for present weather (visibility) and total global radiation. The cloud fraction and height of cloud layers were measured using ceilometer (Vaisala, model CT25K) data. This instrument was at a nearby measurement site, Kenttäröva, at ca. 200 m lower elevation and about 7 km east from Sammaltunturi station.

2.3. Data analyses

The data analyzed here cover the years 2001–2010 for the scattering coefficient, the years 2005–2010 for the absorption coefficient and the years 2004–2010 for the AOD. The data were first quality checked against peculiar events, such as extreme high or low concentrations, which might be caused by an instrument malfunction. The time resolution of the measurements was 5 min. Hourly averages were calculated if more than 50% of the data existed inside the hour in question. The Sammaltunturi station is occasionally inside a cloud. We filtered out all data that had an hourly average visibility lower than 5000 m or the visibility sensor was not functioning properly. The data with the relative humidity inside nephelometer higher than 50% were also removed, as well as the data influenced by instrumental and infrastructural-caused malfunctions. The final data coverage after this pre-selection and quality assurance was about 50%.

The scattering and absorption coefficients are reported at standard conditions for the temperature and pressure, 0 °C and 1013 mbar, respectively. AOD values were based on hourly averages obtained from 5 min resolution data. Boundary layer height was BLH estimated with European Center for Medium-Range Weather Forecasts model (e.g. Korhonen *et al* 2014).

In order to estimate the magnitude of the climate feedback parameter associated with biogenic emissions, we determined the ambient temperature dependence of several measured quantities. For this purpose, the hourly-average measurement data were divided into ambient temperature bins having a width of 1 °C. The average and standard deviation of the selected quantities were calculated for each temperature bin that had more than 50 data points. In case of sulfate, only daily samples were available, so the above procedure was made for the daily-average temperatures with the requirement of having at least 10 data points for each temperature bin. In a comparison between sulfate mass and mass derived from DMPS measurements, daily averages for DMPS values were also used.

We calculated the top-of-the-atmosphere direct radiative effect of the aerosols, DRE, using the following equation (Sheridan and Ogren 1999):

$$\begin{aligned} \text{DRE} = & S_{\text{rad}} \Phi (1 - C_c) \text{TR}_a^2 (1 - R_s)^2 \\ & \times \left[2R_s(1 - \text{SSA}) / (1 - R_s)^2 \right. \\ & \left. - \beta \times \text{SSA} \right] \times \text{AOD}, \end{aligned} \quad (1)$$

where S_{rad} (W m^{-2}) is the incident solar radiation, Φ is the mean daytime value of the secant of the solar zenith angle, C_c is the fractional cloud cover, TR_a (≈ 0.76) is the atmospheric transmissivity, R_s is the surface albedo, SSA is the aerosol single scattering albedo, β is the average upscatter fraction of the aerosol, and AOD is the AOD.

By assuming that the ambient temperature, T , influences only the aerosol loading in equation (1), we may write $\text{DRE} = \alpha \times \text{AOD}(T)$, and strength of the radiative feedback parameter, f , due to the response of the atmospheric aerosol load to temperature increase becomes

$$f_{\text{AOD}} = \frac{\partial \text{DRE}}{\partial T} = \frac{\partial \text{DRE}}{\partial \text{AOD}} \frac{\partial \text{AOD}}{\partial T} \approx \alpha \frac{\partial \text{AOD}}{\partial T}. \quad (2)$$

The contribution of boundary-layer aerosol population to the total AOD is obtained from the relation $\text{AOD}_{\text{BL}} = \sigma_e \times \text{BLH}$, where σ_e is the aerosol extinction coefficient (the sum of aerosol scattering and absorption coefficients) averaged over the boundary layer with the height of BLH. The aerosol extinction coefficient depends on the ambient relative humidity, RH, and can be written as:

$$\sigma_e = g_1(\text{RH})\sigma_s + g_2(\text{RH})\sigma_a, \quad (3)$$

where σ_s and σ_a are the ‘dry’ aerosol scattering and absorption coefficient, respectively, and g_1 and g_2 are the corresponding enhancement factors due to the water uptake by the aerosol. Using these relations, we obtain an alternative expression for f :

$$\begin{aligned} f_{\sigma} / \alpha = & \text{BLH} \left[g_1 \frac{\partial \sigma_s}{\partial T} + g_2 \frac{\partial \sigma_a}{\partial T} \right] \\ & + \text{BLH} \left[\sigma_s \frac{\partial g_1}{\partial T} + \sigma_a \frac{\partial g_2}{\partial T} \right] \\ & + \left[g_1 \sigma_s + g_2 \sigma_a \right] \frac{\partial \text{BLH}}{\partial T}. \end{aligned} \quad (4a)$$

The third term in the right hand side of equation (4a) takes into account the ‘dilution’ of surface-emitted pollutants due to the increase of the BLH with increasing temperatures. In our analysis, we will exclude the contribution of light absorption ($\sigma_a = 0$) in equation (4a) because the influence of BSOA on σ_a is expected to be minor. Because of experimental limitations, we will also neglect the RH dependence of the aerosol scattering coefficient ($g_1 = 1$). These approximations lead to:

$$f_{\sigma} \approx \alpha \left[\text{BLH} \frac{\partial \sigma_s}{\partial T} + \sigma_s \frac{\partial \text{BLH}}{\partial T} \right]. \quad (4b)$$

Equations (2) and (4b) provide us with two alternative ways to estimate the radiative feedback based on the available measurements and, together

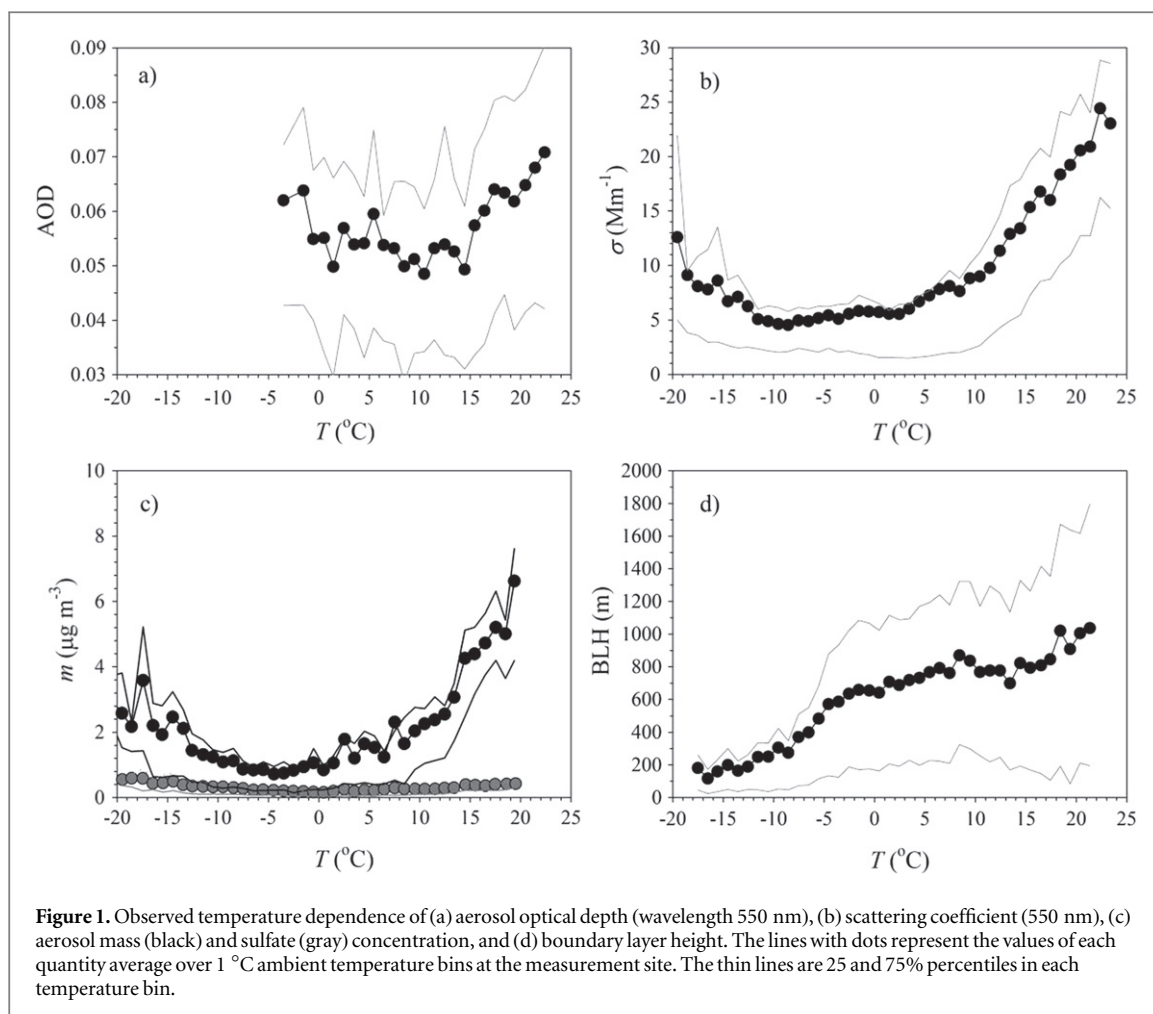


Figure 1. Observed temperature dependence of (a) aerosol optical depth (wavelength 550 nm), (b) scattering coefficient (550 nm), (c) aerosol mass (black) and sulfate (gray) concentration, and (d) boundary layer height. The lines with dots represent the values of each quantity average over 1°C ambient temperature bins at the measurement site. The thin lines are 25 and 75% percentiles in each temperature bin.

with equation (4a), make it possible to get insight into the associated uncertainties.

3. Results and discussion

3.1. Estimated magnitude of the direct radiative feedback

Figure 1 illustrates the temperature dependence of the atmospheric aerosol loading and BLH in our data set. As a general pattern, we observed a broad minimum in the average values of σ_s , submicron aerosol mass and sulfate concentration at temperatures around zero $^{\circ}\text{C}$, a slightly narrower minimum in AOD, and clearly higher values in all these quantities at both lower and higher temperatures. The elevated aerosol concentrations at cold temperatures are due to the enhanced effect of long-range-transported pollution in winter, i.e. Arctic haze, combined with local/regional aerosol emissions associated mainly with residential combustion into the typically shallow boundary layer (Lihavainen *et al* 2015).

At ambient temperatures higher than a few $^{\circ}\text{C}$, a notable increase in the average aerosol loading with an increasing value of T was observed. We hypothesize that this phenomenon is mainly due to enhanced BSOA formation at higher temperatures. Several

pieces of evidence support this view. First, the scattering Ångström exponent increased from the average value of about 1.4 to about 2.0 when the ambient temperature increased from 0 $^{\circ}\text{C}$ to 20 $^{\circ}\text{C}$ (figure 2(a)). This kind of behavior rules out any significant contribution of mineral dust, sea spray or large primary biogenic particles to the enhanced aerosol scattering at higher temperatures. Second, while the average sulfate concentration increased slightly with increasing temperatures when $T > 0^{\circ}\text{C}$, its overall contribution to the aerosol mass increase was minor ($<5\%$, figure 1(c)). Third, the average value of σ_s increased considerably faster with increasing ambient temperatures (140% between 10 and 20 $^{\circ}\text{C}$) than that of σ_a (about 50%, not shown here). These features indicate that while various types of combustion sources contributed to elevated aerosol concentrations at temperatures higher than a few $^{\circ}\text{C}$, their contribution was clearly much lower than that of BSOA. The increased formation of BSOA with increasing ambient temperatures, as observed here, has previously been reported for several other field sites as well (e.g. Tunved *et al* 2006, Leaitch *et al* 2011, Miyazaki *et al* 2012, Ahlm *et al* 2013, Paasonen *et al* 2013, Liao *et al* 2014). In addition, most of the biogenic organic emissions from pine forest (i.e. boreal forest) have been shown to be

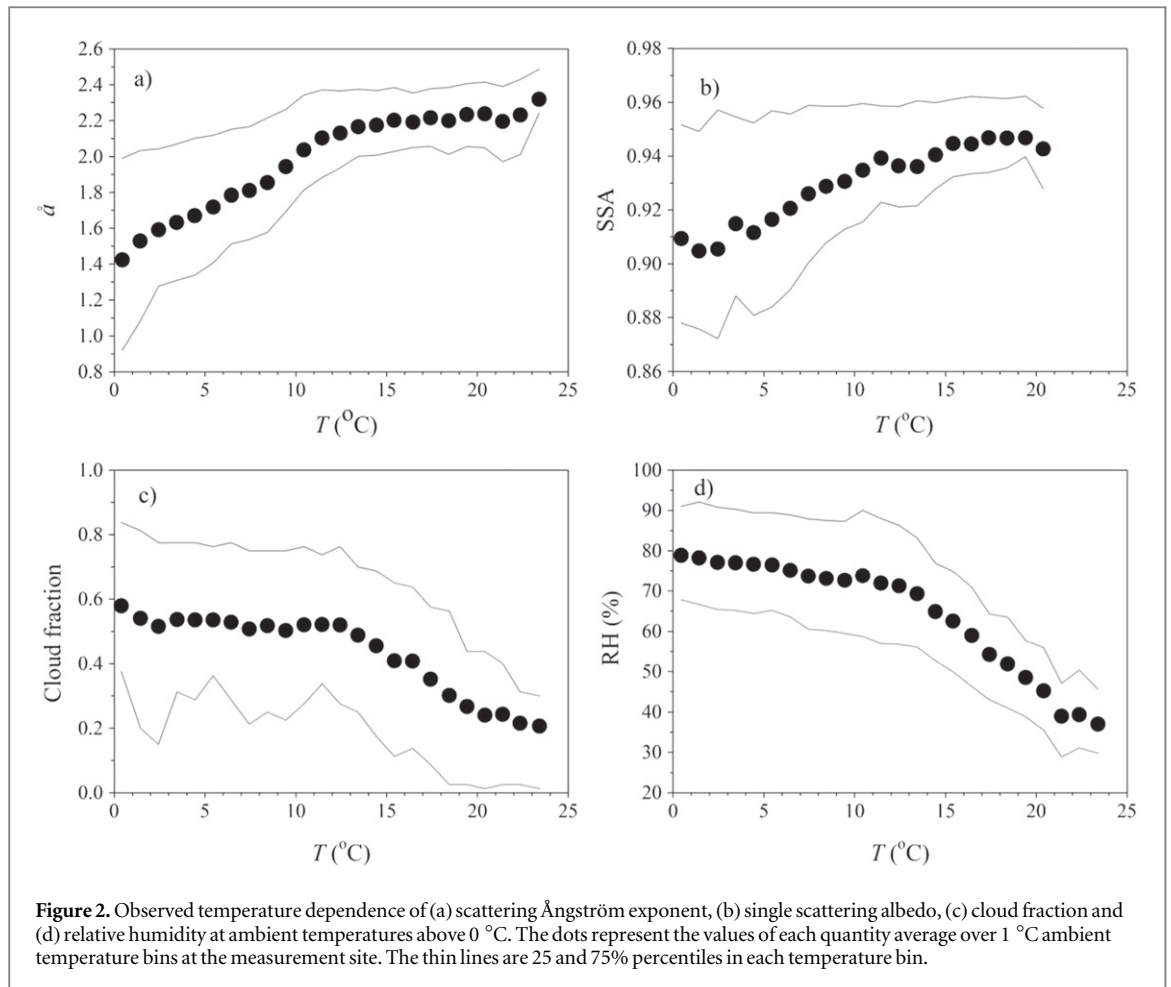


Figure 2. Observed temperature dependence of (a) scattering Ångström exponent, (b) single scattering albedo, (c) cloud fraction and (d) relative humidity at ambient temperatures above 0 °C. The dots represent the values of each quantity average over 1 °C ambient temperature bins at the measurement site. The thin lines are 25 and 75% percentiles in each temperature bin.

temperature and not light dependent (Tarvainen *et al* 2005).

In order to estimate the radiative feedback associated with the temperature-driven BSOA formation, we first assumed that $R_s = 0.1$, $S_{\text{rad}} = 345 \text{ W m}^{-2}$ and $\Phi = 2.9$ in equation (1). These values are good approximations to R_s , S_{rad} and Φ when averaged over the summer period at our measurement site (Lihavainen *et al* 2009). We then selected the temperature range of 10–20 °C and determined the average (\pm STD) values of C_c (0.47 ± 0.31), SSA (0.94 ± 0.03) and β (0.276 ± 0.028) over this temperature range from the measurement data. These values resulted in $\alpha = -60.7 \pm 38.3 \text{ W m}^{-2}$, the large variability of α being mainly due to the highly variable cloud fraction. Next, we made linear fits to the temperatures dependences of AOD, σ_s and BLH between 10 and 20 °C (see figure 1 for the overall temperature dependency of these quantities). The slopes of these fits, combined with α , finally gave $f_{\text{AOD}} = -97 \pm 66 \text{ mW m}^{-2} \text{ K}^{-1}$ and $f_\sigma = -63 \pm 40 \text{ mW m}^{-2} \text{ K}^{-1}$.

3.2. Uncertainties and sensitivity to key assumptions

Here we analyze briefly how sensitive our estimated values of f_{AOD} and f_σ are to our key assumptions. The

first assumption we did in our analysis was that α is constant in equation (2). In our analysis, the only quantity in α that systematically affects the values of either f_{AOD} or f_σ is the apparent temperature dependence of the aerosol single scattering albedo. Based on the observed behavior of SSA (figure 2(a)), we calculated that the magnitude of f_σ was influenced only by about 2% due to the temperature dependency of SSA over the temperature range 10–20 °C. The same was true for f_{AOD} , provided that the ‘dry’ surface-based SSA shown in figure 2(b) is a reasonable proxy for the ‘wet’ SSA averaged over the BL. We may conclude that our estimates for f_{AOD} and f_σ are not sensitive to our assumption $\alpha = \text{constant}$.

Besides overall uncertainties in AOD measurements, an apparent error source for our estimate on f_{AOD} comes from aerosol particles located above the boundary layer that may be totally unrelated to BSOA. Such aerosol particles would influence f_{AOD} if their loading had some systematic dependence on the ambient temperature measured at the surface. The magnitude and sign of such effect cannot be estimated based on our measurements.

The most crucial assumptions in deriving the value of f_σ were that we neglected the contribution of aerosol absorption ($\sigma_a = 0$) and aerosol water uptake ($g_1 = 1$).

Aerosol extinction influences f_σ via both its temperature dependence (the first two terms in the right hand side of equation (4a), or the first term in the right hand side of equation (4b)) and its absolute value (the third term in the right hand side of equation (4a), or the second term in the right hand side of equation (4b)). In our data set, the term including the absolute value of aerosol extinction gave about a 20% contribution to f_σ , so the terms that take into account the temperature dependency of aerosol extinction were clearly more important ones.

Aerosol absorption contributed $6 \pm 3\%$ to the 'dry' aerosol extinction over the temperature range 10–20 °C in our data set (figure 2(b)), and 4% to the increase of the 'dry' aerosol extinction (result not shown here) over the same temperature range. Based on these values and our analysis in the previous paragraph, we may thus conclude that neglecting aerosol absorption decreased the estimated value of f_σ by about 4–5%. This is the maximum percentage by which we may have underestimated the value of f_σ due to the assumption $\sigma_a = 0$, since biogenic SOA is very unlikely to be the only contributor to aerosol absorption in our data set.

Aerosol water uptake influences all the terms in equation (4a). To the first order, f_σ is directly proportional to the value of g_1 . In environments with high sulfate or sea-salt fraction of measured aerosol, g_1 may be larger than 2 at RH > 80% (Zieger *et al* 2013), whereas for aerosols containing more than 90% of organic material, g_1 remains usually below 1.3–1.4 at RH < 80% (Quinn *et al* 2005). Assuming $\partial g_1 / \partial T = 0$ partially compensates the assumption $g_1 = 1$ in equation (4a), since our aerosols tended to have a large organic fraction at higher ambient temperatures (i.e. $\partial g_1 / \partial T < 0$ due to the aerosol composition change). Taken together, we conclude that excluding aerosol water uptake causes a systematic under-prediction of f_σ in our data set. We are not able to quantify this under-prediction, but provide an upper-limit estimate of about 30% for it.

Both cloud fraction and ambient relative humidity decreased considerably over the temperature range 10–20 °C in our data set (figures 2(c) and (d)). We did not include these effects in our feedback calculations, since they are not part of the real radiative feedback associated with the BSOA formation, but rather a sign of some systematic dependency of air mass properties on the ambient temperature. In order to get insight into this issue, we determined 120 h air mass back trajectories for our data set by following the procedure by Lihavainen *et al* (2015). We found that over the temperature range of 10–20 °C, air masses having higher ambient temperatures had, on average, spent longer times over the continent (as opposed to the ocean) before arriving at our measurement site. While explaining the observed patterns of C_c and RH in figure 2, this feature also indicates that the higher BSOA loadings observed at higher ambient

temperatures were not only due to higher biogenic emission rates at elevated temperatures but also due to longer exposure times of the measured air to biogenic emissions. This latter effect causes a positive bias in the estimated values of f_{AOD} and f_σ in our data set, the magnitude of which cannot be quantified using observations alone.

Our estimate for the radiative feedback is sensitive to the temperature range used to calculate the derivatives in equations (2) and (4b), as can be easily seen by looking at figures 1(a) and (b). The temperature range used in our analysis (10–20 °C) is close to that observed in July at our measurement site, the average summer temperature being a few °C lower at this site (Lihavainen *et al* 2015). If we repeat our analysis using the temperature range of 5–15 °C (0–10 °C) instead of 10–20 °C, the value of f_σ will decrease by >50% (>70%). The value of f_{AOD} would decrease even faster.

3.3. Comparison to other studies and large-scale implications

To our knowledge, the only other study that has estimated the direct radiative feedback associated with BSOA is that by Paasonen *et al* (2013). They started their analysis from measured particle number size distributions and, using a few relatively crude assumptions, derived f separately for 11 terrestrial sites ranging from clean boreal forest environments to polluted background sites. When considering all the data measured at temperatures >5 °C, the values of f reported by Paasonen *et al* (2013) ranged from –60 to 6 mW m^{–2} K^{–1} with an overall mean of –30 mW m^{–2} K^{–1}.

Based on earlier results about the radiative forcing by BSOA (Lihavainen *et al* 2009), we may conclude that the direct radiative feedback by BSOA is considerably lower (up to a factor 10) than the feedback due to the first indirect effect of BSOA at our measurement site. How would the situation change in warmer or more polluted environments? Of the locations considered by Paasonen *et al* (2013), the highest feedback due to the indirect effect by BSOA during summer was estimated for Värriö (about –760 mW m^{–2} K^{–1} at ambient temperatures >5 °C), a site with average aerosol properties similar to those in Pallas (Dal Maso *et al* 2008). The strength of this feedback was estimated to be much lower in more polluted environments, as the cloud albedo is less susceptible to aerosol perturbations in more polluted environments (Painemal and Minnis 2012, Spracklen and Rap 2013). Contrary to the indirect radiative effect, the direct radiative effect by BSOA (and thus feedback) is expected to increase linearly with the increasing mass concentration of BSOA. Our previous study has shown that compared with Pallas and Värriö, the strength of BSOA formation is about two times higher in Hyttälä, a boreal forest site approximately 700 km south of both Pallas and

Värriö (Tunved *et al* 2006). Even higher BSOA formation rates have been reported for cases when biogenic emissions are mixed with anthropogenic pollutants (Spracklen *et al* 2011, Xu *et al* 2015). These arguments indicate that the feedback due the direct radiative effect by BSOA might be comparable to, or even larger than, the corresponding feedback due the first indirect radiative effect in such moderately or highly polluted environments that are exposed to biogenic emissions.

4. Concluding remarks

This is the first study in which the direct radiative feedback parameter associated with BSOA formation has been derived directly from optical aerosol measurements. Our two independent estimates ($f_{\text{AOD}} = -97 \pm 66 \text{ mW m}^{-2} \text{ K}^{-1}$ and $f_{\sigma} = -63 \pm 40 \text{ mW m}^{-2} \text{ K}^{-1}$) represent upper-limit values for this feedback over the summer period at our site, because the temperature range used in our analysis was somewhat higher than the typical summer temperatures at our site and because the observed temperature-dependent BSOA formation was evidently biased by air mass transport effects. Compared to the measurement site considered here, the magnitude of f is expected to be larger at lower latitudes where biogenic emissions tend to be stronger. Even larger values of f are plausible in regions where biogenic emissions are mixed with anthropogenic pollution. Most importantly, f may be comparable to, or even larger than, the corresponding feedback due the first BSOA indirect effect over vast continental regions.

It should be noted that the observed temperature-dependence of BSOA formation may not be representative of what is taking place in the future climate system. This is firstly because the short- and long-term effects of the ambient temperature on atmospheric BSOA loadings might be quite different. For example, temperature changes almost certainly affect the amount and type of vegetation responsible for BSOA precursor emissions in both Arctic and Boreal environments over the climate-relevant time scales (e.g. Wang *et al* 2011, Pearson *et al* 2013, Buermann *et al* 2014). This feature is not taken into account in our analysis. Secondly, also components other than temperature in the climate system influence atmospheric BSOA. These include the future increase of the ambient CO_2 concentration and yet poorly-quantified future changes in extreme weather conditions, precipitation patterns and atmospheric chemistry (Grote and Niinemets 2008, Guenther *et al* 2012).

Finally, future changes in the atmospheric BSOA and their precursor loadings, either due to changing climate or land use, may trigger additional feedback mechanisms that lead to considerable radiative effects. Such feedbacks might arise, for example, via changes in atmospheric chemistry, in the ratio between diffuse

and direct radiation entering the Earth's surface, or in the carbon and water cycles (e.g. Carslaw *et al* 2010, Cirino *et al* 2014, Kulmala *et al* 2014, Unger 2014). These issues bring up the need to extend these kind of analyses to other continental sites from which long-term observations are available, to complement such analyses with model simulations whenever feasible, and to look for additional feedback mechanisms that might be relevant for the climate system.

Acknowledgments

This work was supported by the Academy of Finland as part of the Centre of Excellence program (project no 1118615) and Arctic Absorbing Aerosols and Albedo of Snow (project no. 3162), EU LIFE+ project MACEB (project no. LIFE09 ENV/FI/000572) and Nordic research and innovation initiative Cryosphere–Atmosphere Interactions in a Changing Arctic Climate (CRAICC).

References

- Aaltonen V, Lihavainen H, Kerminen V-M, Komppula M, Hatakka J, Eneroth K, Kulmala M and Viisanen Y 2006 Measurements of optical properties of atmospheric aerosols in Northern Finland *Atmos. Chem. Phys.* **6** 1155–64
- Aaltonen V, Rodriguez E, Kazadzis S, Arola A, Amiridis V, Lihavainen H and de Leeuw G 2012 On the variation of aerosol properties over Finland based on the optical columnar measurements *Atmos. Res.* **116** 46–55
- Ahlm L *et al* 2013 Temperature-dependent accumulation mode particle and cloud nuclei concentrations from biogenic sources during WACS 2010 *Atmos. Chem. Phys.* **13** 3393–407
- Anderson T L and Ogren J 1998 Determining aerosol radiative properties using the TSI 3563 Integrating Nephelometer *Aerosol Sci. Technol.* **29** 57–69
- Boucher O *et al* 2013 Clouds and aerosols *Climate Change 2013: The Physical Science Basis. Contribution of Working Group I to the Fifth Assessment Report of the Intergovernmental Panel on Climate Change* ed T F Stocke *et al* (Cambridge: Cambridge University Press)
- Buermann W, Parida B, Jung M, Tucker C J and Reichstein M 2014 Recent shift in Eurasian boreal forest greening response may be associated with warmer and drier summers *Geophys. Res. Lett.* **41** 1995–2002
- Carslaw K S, Boucher O, Spracklen D V, Mann G W, Rae J G L, Woodward S and Kulmala M 2010 A review of natural aerosol interactions and feedbacks within the Earth system *Atmos. Chem. Phys.* **10** 1701–37
- Carslaw K S *et al* 2013 Large contribution of natural aerosols to uncertainty in indirect radiative forcing *Nature* **503** 67–71
- Cirino G G, Souza R A F, Adams D K and Artaxo P 2014 The effect of atmospheric aerosol particles and clouds on net ecosystem exchange in the Amazon *Atmos. Chem. Phys.* **14** 6523–43
- Dal Maso M, Hyvärinen A, Komppula M, Tunved P, Kerminen V-M, Lihavainen H, Viisanen Y, Hansson H-C and Kulmala M 2008 Annual and interannual variation in boreal forest aerosol particle number and volume concentration and their connection to particle formation *Tellus B* **60** 495–508
- Goto D, Takemura T and Nakajima T 2008 Importance of global aerosol modeling including secondary organic aerosol from monoterpene *J. Geophys. Res.* **113** D07205
- Grote R and Niinemets Ü 2008 Modeling volatile isoprenoid emissions—a story with split ends *Plant Biol.* **10** 8–28
- Guenther A B, Jiang X, Heald C L, Sakulyanontvittaya T, Duhl T, Emmons L K and Wang X 2012 The model of emissions of

- gases and aerosols from nature version 2.1. MEGAN 2.1: an extended and updated framework for modeling biogenic emissions *Geosci. Model Dev.* **5** 1471–92
- Hatakka J *et al* 2003 Overview of the atmospheric research activities and results at Pallas GAW station *Boreal Environ. Res.* **8** 365–83
- Komppula M, Lihavainen H, Hatakka J, Paatero J, Aalto P, Kulmala M and Viisanen Y 2003 Observations of new particle formation and size distributions at two different heights and surroundings in subarctic area in northern Finland *J. Geophys. Res.* **108D9** 4295
- Korhonen K *et al* 2014 Atmospheric boundary layer top height in South Africa: measurements with lidar and radiosonde compared to three atmospheric models *Atmos. Chem. Phys.* **14** 4263–78
- Kulmala M *et al* 2004 A new feedback mechanism linking forests, aerosols, and climate *Atmos. Chem. Phys.* **4** 557–62
- Kulmala M *et al* 2014 CO₂ induced terrestrial climate feedback mechanism: from carbon sink to aerosol source and back *Boreal Environ. Res.* **19** (suppl. B) 122–31
- Leitch W R *et al* 2011 Temperature response of the submicron organic aerosol from temperate forests *Atmos. Environ.* **45** 6696–704
- Lihavainen H, Hyvärinen A, Asmi E, Hatakka J and Viisanen Y 2015 Long-term variability of aerosol optical properties in Northern Finland *Boreal Environ. Res.* **20** 526–41
- Lihavainen H, Kerminen V-M, Tunved P, Aaltonen V, Arola A, Hatakka J, Hyvärinen A and Viisanen Y 2009 Observational signature of the direct radiative effect by natural boreal forest aerosols and its relation to the corresponding first indirect effect *J. Geophys. Res.* **114** D20206
- Liao L, Kerminen V-M, Boy M, Kulmala M and Dal Maso M 2014 Temperature influence on the natural aerosol budget over boreal forests *Atmos. Chem. Phys.* **14** 8295–308
- Miyazaki Y, Jung J, Fu P, Mizoguchi Y, Yamanoi K and Kawamura K 2012 Evidence formation of submicrometer water-soluble organic aerosols at a deciduous forest site in northern Japan in summer *J. Geophys. Res.* **117** D19213
- O'Donnell D, Tsigaridis K and Feichter J. 2011 Estimating the direct and indirect effects of secondary organic aerosols using ECHAM-HAM *Atmos. Chem. Phys.* **11** 8635–59
- Paasonen P *et al* 2013 Warming-induced increase in aerosol number concentration likely to moderate climate change *Nat. Geosci.* **6** 438–42
- Painemal D and Minnis P 2012 On the dependence of albedo on cloud microphysics over marine stratocumulus clouds regimes determined from Clouds and Earth's Radiant Energy System CERES data *J. Geophys. Res.* **117** D06203
- Pearson R G, Philips S J, Lorant M M, Beck P S A, Damoulas T, Knight S J and Goetz S J 2013 Shifts in Arctic vegetation and associated feedbacks under climate change *Nat. Clim. Change* **3** 673–77
- Quinn P K *et al* 2005 Impact of particulate organic matter on the relative humidity dependence of light scattering: a simplified parameterization *Geophys. Res. Lett.* **32** L22809
- Rap A, Scott C E, Spracklen D V, Bellouin N, Forster P M, Carslaw K S, Schmidt A and Mann G 2013 Natural aerosol direct and indirect radiative effects *Geophys. Res. Lett.* **40** 3297–301
- Scott C E *et al* 2014 The direct and indirect radiative effects of biogenic secondary organic aerosol *Atmos. Chem. Phys.* **14** 447–70
- Sheridan P J and Ogren J A 1999 Observations of the vertical and regional variability of aerosol optical properties over central and eastern North America *J. Geophys. Res.* **104** 793–805
- Smirnov A, Holben B N, Eck T F, Dubovik O and Slutsker I 2000 Cloud screening and quality control algorithms for AERONET database *Remote Sens. Environ.* **73** 337–49
- Spracklen D V, Bonn B and Carslaw K S 2008 Boreal forests, aerosols and the impacts on clouds and climate *Phil. Trans. R. Soc. A* **266** 1–11
- Spracklen D V and Rap A 2013 Natural aerosol-climate feedbacks suppressed by anthropogenic aerosol *Geophys. Res. Lett.* **40** 5316–19
- Spracklen D V *et al* 2011 Aerosol mass constraint on the global secondary organic aerosol budget *Atmos. Chem. Phys.* **11** 12109–36
- Tarvainen V, Hakola H, Hellén H, Bäck J, Hari P and Kulmala M 2005 *Atmos. Chem. Phys.* **5** 989–98
- Tunved P *et al* 2006 High natural aerosol loading over boreal forests *Science* **312** 261–3
- Tunved P, Ström J, Kulmala M, Kerminen V-M, Dal Maso M, Svenningsson B, Lunder C and Hansson H-C 2008 The natural aerosol over Northern Europe and its relation to anthropogenic emissions—implications of important climate feedbacks *Tellus B* **60** 473–84
- Unger N 2014 On the role of plant volatiles in anthropogenic global climate change *Geophys. Res. Lett.* **41** 8563–69
- Wang X, Piao S, Ciais P, Li J, Friedlingstein P, Koven C and Chen P 2011 Spring temperature change and its implication in the change of vegetation growth in North America from 1982 to 2006 *Proc. Natl Acad. Sci. USA* **108** 1240–45
- Weingartner E, Saathoff H, Schnaiter M, Streit N, Bitnar B and Baltensperger U 2003 Absorption of light by soot particles: determination of the absorption coefficient by means of aethalometers *J. Aerosol Sci.* **34** 1445–63
- Xu L *et al* 2015 Effects of anthropogenic emissions on aerosol formation from isoprene and monoterpenes in the southeastern United States *Proc. Natl Acad. Sci. USA* **112** 37–42
- Zieger P, Fierz-Schmidhauser R, Weingartner E and Baltensperger U 2013 Effects of relative humidity on aerosol light scattering: results from different European sites *Atmos. Chem. Phys.* **13** 10609–31